



LQR Combined with Fuzzy Control for 2-DOF Planar Robot Trajectories

A. Hernandez-Pineda¹, I. Bezerra-Viana¹ ^a, M. Marques-Simoes¹ ^b and F. Bezerra Carvalho²

¹Programa de Pós-Graduação em Engenharia Elétrica e Computação, Universidade Federal do Ceará,
Rua Coronel Estandeu Frota-563, Sobral, Brazil

²Programa de Pós-Graduação em Engenharia Elétrica e Computação, Universidade Federal do Ceará, Sobral, Brazil

Keywords: Planar Robot Manipulator, LQR, Fuzzy Logic, Trajectory Control.


Abstract: Some tasks of robotic manipulators are performed using control techniques for trajectory tracking. These techniques ensure that the existing steady-state error between the desired and executed trajectories are close to zero. This work proposes a hybrid control scheme that enhances a traditional control approach with computational tuning optimization. The Linear Quadratic Regulator (LQR) controller is implemented by manipulating the state variables of the plant to be controlled. The optimization of this controller is related to the weighting variables of the cost function. Computational tuning using fuzzy logic is applied to adjust the weighting variables of LQR. The results demonstrate that the hybrid control optimal performance outperformed the traditional LQR controller in the trajectory following task for the two-degree-of-freedom planar robotic manipulator.


1 INTRODUCTION

Robotics was developed with the intention of automating repetitive, complex, or precise tasks. Industries with robust processes found in robotics an alternative for hazardous activities, avoiding risks for their workers. Precision features offered by robotics are valued in the medical field and in microcomponent production. Operations and tasks like those previously mentioned are carried out by robots through high-precision control strategies. Such strategies are implemented in anthropomorphic manipulators to correct the error difference between the obtained and desired trajectories. The precision and stability demands in robot trajectory tracking has led to innovative control methodologies that rely or not on the robot dynamic model.

In the first group, controllers such as the Computed Torque Controller (CTC) (García et al., 2018), the Sliding Mode Controller (SMC) (Nguyen, 2019), the Linear Quadratic Regulator (LQR) Controller (Mahil and Al-Durra, 2016), and the Model Predictive Controller (Wahrburg and Listmann, 2016) Are not frequently used in robotic manipulators due to its highly nonlinear model. In contrast, con-

trollers that depend of plant dynamic model, such as the Proportional-Integral-Derivative (PID) Controller (Kelly et al., 2005), Fuzzy Logic Controller (Ho et al., 2007), Kinematic Analyzer via Neural Network (Shah et al., 2011) and the hybrid controller of computerized torque with fuzzy logic (Song et al., 2005) Are robust to the nonlinearity of robotics but most of them require high computational resources. There are approaches that have been proposed to address nonlinearity in robotic controlling with low computational resources, as the Robust Computed Torque Controller (Kardoš, 2019), Robust Controller via Neural Network Compensation (Li et al., 2005), and Computed Torque Controller with Fuzzy Tuning (Pizarro-Lerma et al., 2018). This third group comprises hybrid controllers with low computational resources to determine the uncertainties presented by the nonlinearity found in robotic systems. Precisely the non-linearity of these MIMOS (multiple input - multiple output) systems is the factor that makes the control and functionality of robotic systems complex (Kumar et al., 2023). In this context, this article proposes a hybrid strategy for anthropomorphic manipulators control based on the optimization, with computational tuning, of a LQR controller. The latter is implemented through the linearized dynamic model of the plant, and the performance of this controller is linked to the feedback matrix, which is calculated using the

^a  <https://orcid.org/0000-0002-0009-8330>

^b  <https://orcid.org/0000-0002-7590-9898>

cost function values. Applying fuzzy logic to find the weighting values of the cost function, it becomes possible to create a hybrid controller for trajectory tracking (Kudinov et al., 2020).

Methodologies based on fuzzy logic control are capable of operating alongside the nonlinearities of robotic systems, as presented in the work of (Sun et al., 2023), thus improving the trajectory performance of robotic arms. The difficulties of nonlinearity have also been discussed with hybrid methods of fuzzy logic systems by Lyapunov stability analysis (An et al., 2023). In both works an implementation is presented simply to implement fuzzy logic control to complex systems. Furthermore, the openness of this control methodology to be applied in tuning methods is evident, making robust and reliable controls.

As a contribution, this article brings LQR-FL as a proposal for controlling planar robotic manipulators trajectories, and compares its performance to the classic LQR controller.

The structure of this work is as follows. Section II contains the dynamics of the system in its state space form. Section III presents the LQR controller and its association with fuzzy logic. Section IV presents the evaluation of the controllers and the comparison of the results. Section V is dedicated to the conclusions.

2 DYNAMIC MODEL

The motion dynamics of the 2-DOF Planar Manipulator is as follow:

$$M(\theta)\ddot{\theta} + V(\theta, \dot{\theta}) + g = \tau \quad (1)$$

The dynamic analysis of energies is carried out through the Lagrangian:

$$L = KE - PE \quad (2)$$

where, KE is the kinetic energy and PE is system potential energy. The Lagrangian is used to derive the dynamic model of the planar manipulator robot shown in Figure 1, which is composed by masses m_1 and m_2 , lengths l_1 and l_2 , inertia tensors I_{z1} and I_{z2} , and center of gravity r_1 and r_2 .

For each of the manipulator's axes, the description of linear displacement relative to the x/y coordinates of the operating area is given by:

$$P_1 = \begin{bmatrix} x_1 \\ y_1 \\ z_1 \end{bmatrix} = \begin{bmatrix} l_1 \sin(\theta_1) \\ l_1 \cos(\theta_1) \\ 0 \end{bmatrix} \quad (3)$$

$$P_2 = \begin{bmatrix} x_2 \\ y_2 \\ z_2 \end{bmatrix} = \begin{bmatrix} l_1 \sin(\theta_1) + l_2 \sin(\theta_1 + \theta_2) \\ l_1 \cos(\theta_1) + l_2 \cos(\theta_1 + \theta_2) \\ 0 \end{bmatrix} \quad (4)$$

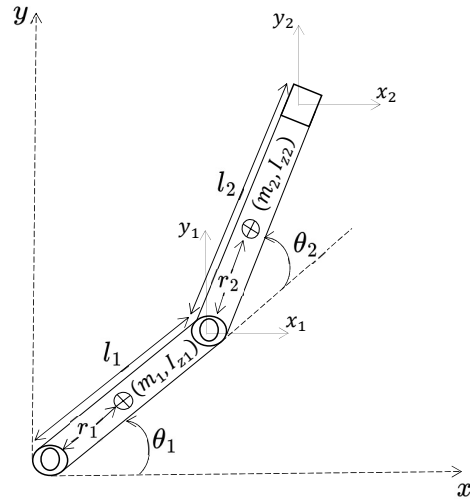


Figure 1: Two degrees of freedom planar manipulator.

The kinetic energy equation is:

$$KE = \frac{1}{2}m_1v_1^2 + \frac{1}{2}I_{z1}\dot{\theta}_1^2 + \frac{1}{2}m_2v_2^2 + \frac{1}{2}I_{z2}\dot{\theta}_2^2 \quad (5)$$

Replacing velocities v_1 and v_2 with positions derivatives of Equations 3 and 4, yields:

$$KE = \frac{1}{2}m_1(\dot{x}_1^2 + \dot{y}_1^2) + \frac{1}{2}I_{z1}\dot{\theta}_1^2 + \frac{1}{2}m_2(\dot{x}_2^2 + \dot{y}_2^2) + \frac{1}{2}I_{z2}\dot{\theta}_2^2, \quad (6)$$

$$PE = m_1g(z_1^2) + m_2g(z_2^2). \quad (7)$$

and replacing KE and PE of Equations 6 and 7 in Equation 2 results:

$$L = \frac{1}{2}I_{z1}[m_1r_1^2 + m_2(l_1^2 + r_2^2 + 2l_1r_2C_2)]\dot{\theta}_1^2 + \frac{1}{2}I_{z2}[m_2r_2^2]\dot{\theta}_2^2 + \frac{1}{2}[m_22r_2(l_1C_2 + d_2)]\dot{\theta}_1\dot{\theta}_2 - g(0) \quad (8)$$

Applying partial derivatives to the Lagrangian leads to the dynamic model of forces:

$$\begin{bmatrix} M_{11} & M_{12} \\ M_{21} & M_{22} \end{bmatrix} \begin{bmatrix} \ddot{\theta}_1 \\ \ddot{\theta}_2 \end{bmatrix} + \begin{bmatrix} V_{11} & V_{12} \\ V_{21} & V_{22} \end{bmatrix} \begin{bmatrix} \dot{\theta}_1 \\ \dot{\theta}_2 \end{bmatrix} + \begin{bmatrix} g_1 \\ g_2 \end{bmatrix} = \begin{bmatrix} \tau_1 \\ \tau_2 \end{bmatrix} \quad (9)$$

where,

$$\begin{aligned} M_{11} &= m_1r_1^2 + m_2[l_1^2 + r_2^2 + 2l_1r_2 \cos(\theta_2)] + I_{z1} + I_{z2}, \\ M_{12} &= m_2[r_2^2 + l_1r_2 \cos(\theta_2)] + I_{z2}, \\ M_{21} &= m_2[r_2^2 + l_1r_2 \cos(\theta_2)] + I_{z2}, \\ M_{22} &= m_2r_2^2 + I_{z2}, \\ V_{11} &= -m_2l_1r_2 \sin(\theta_2)\dot{\theta}_2, \\ V_{12} &= -m_2l_1r_2 \sin(\theta_2)(\dot{\theta}_1 + \dot{\theta}_2), \\ V_{21} &= -m_2l_1r_2 \sin(\theta_2)\dot{\theta}_1, \end{aligned}$$

$$\begin{aligned} V_{22} &= 0, \\ g_1 &= 0, \\ g_2 &= 0. \end{aligned}$$

This planar manipulator has no vertical movements; thus, the gravity value is zero. A system in state space is represented by the expression :

$$\dot{x} = Ax + Bu. \quad (10)$$

The Equation 9, which represents the torque exerted on the joints of the plane manipulator, is not linear. To express this system as a state space model, the state variables are considered as follows:

$$x_1 = \theta_1, x_2 = \theta_2, x_3 = \dot{\theta}_1, x_4 = \dot{\theta}_2, \quad (11)$$

$$\dot{x}_1 = \dot{\theta}_1, \dot{x}_2 = \dot{\theta}_2, \dot{x}_3 = \ddot{\theta}_1, \dot{x}_4 = \ddot{\theta}_2. \quad (12)$$

These are rewritten and associated with the existing torque equations for the joints:

$$\dot{x}_1 = x_3, \quad (13)$$

$$\dot{x}_2 = x_4, \quad (14)$$

$$\begin{aligned} \dot{x}_3(m_2 l_1^2 + 2m_2 C_2 l_1 r_2 + I_{z1} + I_{z2}) = \\ \tau_1 - (m_2 r_2^2 + l_1 m_2 C_2 r_2 + I_{z2}) \ddot{\theta}_2 \\ + l_1 m_2 r_2 \dot{\theta}_2 S_2 (\dot{\theta}_1 + \dot{\theta}_2) + l_1 m_2 r_2 \dot{\theta}_1 \theta_2 S_2, \end{aligned} \quad (15)$$

$$\begin{aligned} \dot{x}_4(m_2 r_2 + I_{z2}) = -\tau_1 + m_2 r_2^2 + (l_1 m_2 S_2) \dot{\theta}_1^2 r_2 \\ + I_{z2} + \ddot{\theta}_1 + (l_1 m_2 r_2 \dot{\theta}_1 C_2) \ddot{\theta}_1. \end{aligned} \quad (16)$$

The first-order Taylor series expansion of the dynamic Equations 13, 14, 15, and 16, results in the dynamic matrices A and B:

$$A = \begin{bmatrix} 0 & 0 & 1 & 0 \\ 0 & 0 & 0 & 1 \\ 0 & A_{32} & A_{33} & A_{34} \\ 0 & A_{42} & A_{43} & 0 \end{bmatrix}, \quad (17)$$

where,

$$\begin{aligned} A_{32} &= \frac{\sigma_2 + l_1 m_2 r_2 \dot{\theta}_2 \cos(\theta_2) (\dot{\theta}_1 + \dot{\theta}_2) + l_1 m_2 r_2 \dot{\theta}_1 \dot{\theta}_2 \cos(\theta_2)}{\sigma_1} \\ &- \left(\frac{6I_{z2}}{5} - \tau_1 + \frac{6m_2 r_2^2}{5} + \frac{6l_1 m_2 r_2 \cos(\theta_2)}{5} \right) \\ &- l_1 m_2 r_2 \dot{\theta}_2 \sin(\theta_2) (\dot{\theta}_1 + \dot{\theta}_2) - l_1 m_2 r_2 \dot{\theta}_1 \dot{\theta}_2 \sin(\theta_2) \\ &\frac{2l_1 m_2 r_2 \sin(\theta_2)}{\sigma_1^2} \end{aligned}$$

$$A_{33} = \frac{2l_1 m_2 r_2 \dot{\theta}_2 \sin(\theta_2)}{\sigma_1}$$

$$A_{42} = \frac{\sigma_2 - l_1 m_2 r_2 \dot{\theta}_1^2 \cos(\theta_2)}{\sigma_3}$$

$$A_{43} = -\frac{2l_1 m_2 r_2 \dot{\theta}_1 \sin(\theta_2)}{\sigma_3}$$

$$\sigma_1 = m_2 l_1^2 + 2m_2 \cos(\theta_2) l_1 r_2 + m_1 r_1^2 + m_2 r_2^2 + I_{z1} + I_{z2}$$

$$\sigma_2 = \frac{6l_1 m_2 r_2 \sin(\theta_2)}{5}$$

$$\sigma_3 = m_2 r_2^2 + I_{z2}$$

$$B = \begin{bmatrix} 0 & 0 \\ 0 & 0 \\ B_{31} & 0 \\ 0 & B_{42} \end{bmatrix}. \quad (18)$$

where,

$$B_{31} = \frac{1}{m_2 l_1^2 + 2m_2 \cos(\theta_2) l_1 r_2 + m_1 r_1^2 + m_2 r_2^2 + I_{z1} + I_{z2}}$$

$$B_{42} = \frac{1}{m_2 r_2^2 + I_{z2}}$$

3 CONTROLLER DESIGN

Nonlinearity leads to complex dynamic modeling in robotic systems that challenges to design controllers for the trajectories executed by the robot. LQR was chosen in the design of 2-DOF planar manipulator trajectory controller, since this controller addresses non-linearity issues linearizing the state spaces (Teng Fong et al., 2015), (Lee et al., 2021).

For the adjustment techniques of the fuzzy logic controller, there are different options that are chosen according to the complexity and characteristics of the system. One of the most common techniques is optimization based on heuristics, such as gray wolf optimization (GWO) implemented in the (Bojan-Dragos et al., 2021). Also included in the set of heuristics are optimization by genetic algorithms (GA) and particle swarm optimization presented in (Kumar et al., 2023). Them also cites more traditional techniques for the adjustment of fuzzy controllers such as the Takagi and Sugeno adjustment or the Mamdani adjustment. This last adjustment technique to obtain the relevant functions and fuzzification rules are used in this work, because its methodology is obtained from systems in state space.

3.1 LQR Controller

The LQR controller is designed using the state space model obtained in Equations 17 and 18. The calculation of the gain satisfies the following the equation:

$$K = R^{-1} B^T P. \quad (19)$$

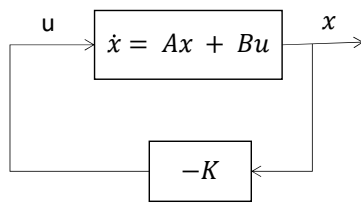


Figure 2: Optimal Regulatory System.

in equation 19, B is the input vector, R is the weighting matrix and P is the Riccati matrix. The R matrix is filled with ones in its initialization, and its solution follows:

$$A^T P + PA + Q - PBR^{-1}P = 0. \quad (20)$$

The weighting matrix Q is given by,

$$Q = C^T C. \quad (21)$$

An optimal regulator system, can be designed accordingly to the Figure 2 (Ogata, 2010).

3.2 LQR-FL Controller

The creation of LQR-FL controller stems from the premise of having an LQR controller implemented in the plant to be controlled. Figure 3 illustrates that fuzzy logic operates within a feedback loop parallel to the operation of the base controller.

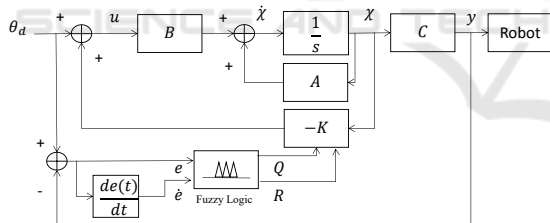


Figure 3: LQR control scheme using Fuzzy Logic.

This control methodology, when implemented into planar manipulator trajectory control scheme, takes as input the desired angular position calculated through inverse kinematics. These controller determine the joint positions to execute the desired trajectory.

The structure of the fuzzy controller, depicted in Figure 4 employs membership functions (MFs) considering as inputs the error between the desired and actual joint position e and its derivative \dot{e} . Meanwhile, the MFs output are the elements of the main diagonal of the matrix Q matrix and the optimal value of R .

The MFs input e and \dot{e} have different operating ranges, yet the triangular and trapezoidal shapes of their linguistic sets coincide, as depicted in Figure

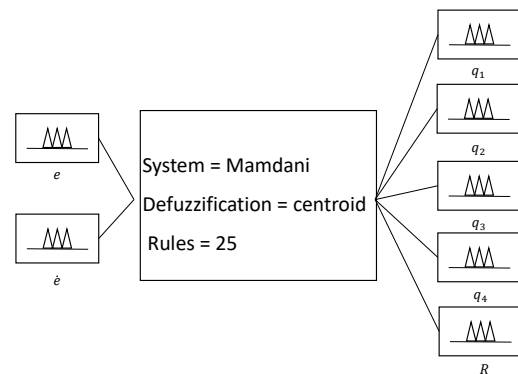


Figure 4: Fuzzy controller structure.

5. The proportionality of the linguistic sets negative big (NB), negative medium (NM), zero (Z), positive medium (PM) and positive big (PB) is adjustable to obtain precise information in the inputs.

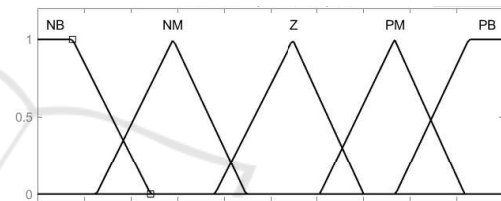


Figure 5: Membership functions of input variables.

The structure of the MFs shown in Figure 6 is implemented in the five outputs of the fuzzy controller. It's evident that these output MFs are a simplified version of the input MFs. The linguistic groups composing them are: small (S), medium (M), Big (B). Each of these output MFs differs in the operating range and the proportionality of each of the sets comprising them.

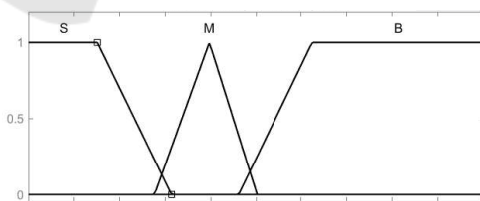


Figure 6: Membership functions of input variables.

The fuzzy controller obtains the output values through decisions that apply the rule base to the input values it is receiving. Table 1. was constructed based on the proposed controller in (Bekkar and Ferrous, 2023).

In the Table 1, position error input values as vertical values. The horizontal of the table is related to the rate of change of value. From this association, the twenty-five operating rules of the fuzzy block

Table 1: Rule base.

q_1, q_2, q_3, q_4 *R	In. (\dot{e})				
	NB	NM	Z	PM	PB
In.(e)					
NB	S,B,M,M *B	M,M,M,M *M	S,S,B,B *B	B,M,S,S *S	B,M,S,S *S
NM	B,B,S,M *S	B,M,S,M *S	M,M,S,M *S	B,M,S,M *S	B,M,S,M *S
Z	M,B,M,S *M	B,B,S,S *M	S,S,M,M *B	B,B,S,S *M	M,B,M,S *M
PM	B,M,S,M *S	B,M,S,M *S	M,M,S,M *S	B,M,S,M *S	B,B,B,S,M *S
PB	B,M,S,S *S	B,M,S,S *S	S,S,B,B *B	M,M,M,M *M	S,B,M,M *B

are obtained. As a result, it is obtained the value of (q_1, q_2, q_3, q_4) and (R).

4 RESULTS AND SIMULATION

In this study, trajectory control simulation is conducted based on the model of a robotic arm shown in Figure 1, The parameters of this two-degree-of-freedom manipulator are those outlined in Table 2.

To design the LQR-FL controller, the parameters in Table 3 are provided. The ranges of the input and output membership functions are specified.

Table 2: Two degrees of freedom planar manipulator parameter values.

Parameter	Value	Units
l_1	0.26	m
l_2	0.38	m
r_1	0.13	m
r_2	0.19	m
m_1	0.53	kg
m_2	0.33	kg
I_{z1}	0.013	$kg * m^2$
I_{z2}	0.016	$kg * m^2$
g	0.	m/s^2

4.1 Controller Parameters

The LQR controller is tuned choosing the weighing the matrix as, $\theta_1=0$, $\theta_2=0$, $\dot{\theta}_1=0$, $\dot{\theta}_2=0$, $Q=\text{diag}[1 \ 1 \ 0 \ 0]$ e $R=[1]$.

Therefore, both controllers are set to operate with the dynamic input arrays of Equations 22 and 23, and the output array of Equation 24.

$$A = \begin{bmatrix} 0 & 0 & 1 & 0 \\ 0 & 0 & 0 & 1 \\ 0 & 0.56 & 0 & 0 \\ 0 & -0.69 & 0 & 0 \end{bmatrix} \quad (22)$$

$$B = \begin{bmatrix} 0 & 0 \\ 0 & 0 \\ 9.42 & 0 \\ 0 & 34.94 \end{bmatrix} \quad (23)$$

$$C = \begin{bmatrix} 1 & 0 & 0 & 0 \\ 0 & 1 & 0 & 0 \end{bmatrix} \quad (24)$$

4.2 Transient Response Analysis

The system has as inputs the unit impulse values for each of the joints of the kinematic chain of the planar manipulator. Controllers having this type of inputs can be evaluated through transient response characteristics. The Table 4 contains the parameters of delay time (td), rise time (tr), peak time (tp) and accommodation time (ts).

Table 4, shows that both controllers comply with the desired positioning with respect to the input value received. Showing a difference in the reduction of time by the LQR-FL hybrid controller to reach the desired position. The speed graphs for the LQR-FL and LQR controllers are shown in Figures 7a and 7b respectively. It agree with the fact that the speeds executed in the LQR-FL controller are faster.

Figure 7c and 7d graphs represents shorter travel times with higher energy peaks for each of the joints in the system. The higher energy peaks obtained with the LQR-FL controller are the effect of better control of the system energy for the same movement pressure due to a computational tuning of the values of the weighting matrices.

Table 3: LQR-FL Membership Features.

In / Out	Fuzzy values obtained	Range of M.F.
Error	(e)	$(-1.2, 1.25)$
Change rate	(\dot{e})	$(-2.0, 2.25)$
$Q = \begin{bmatrix} q_1 & 0 & 0 & 0 \\ 0 & q_2 & 0 & 0 \\ 0 & 0 & q_3 & 0 \\ 0 & 0 & 0 & q_4 \end{bmatrix}$	$\begin{bmatrix} q_1 \\ q_2 \\ q_3 \\ q_4 \end{bmatrix}$	$\begin{bmatrix} (0.98, 1.21) \\ (1.0, 1.1) \\ (0.05, 0.3) \\ (0.1, 0.4) \end{bmatrix}$
R	R	$(0.8, 0.95)$

Table 4: Transient response analysis.

Joint	In	real value	td	tr	tp	ts
n°	deg	deg	s	s	s	s
LQR-1	75	75.1	0.9	4	5	6
LQR-2	45	44.8	0.9	4	6	6.5
LQR-FL/1	75	75.1	0.5	1.8	2	2
LQR-FL/2	45	44.5	0.4	1.5	2.5	2.5

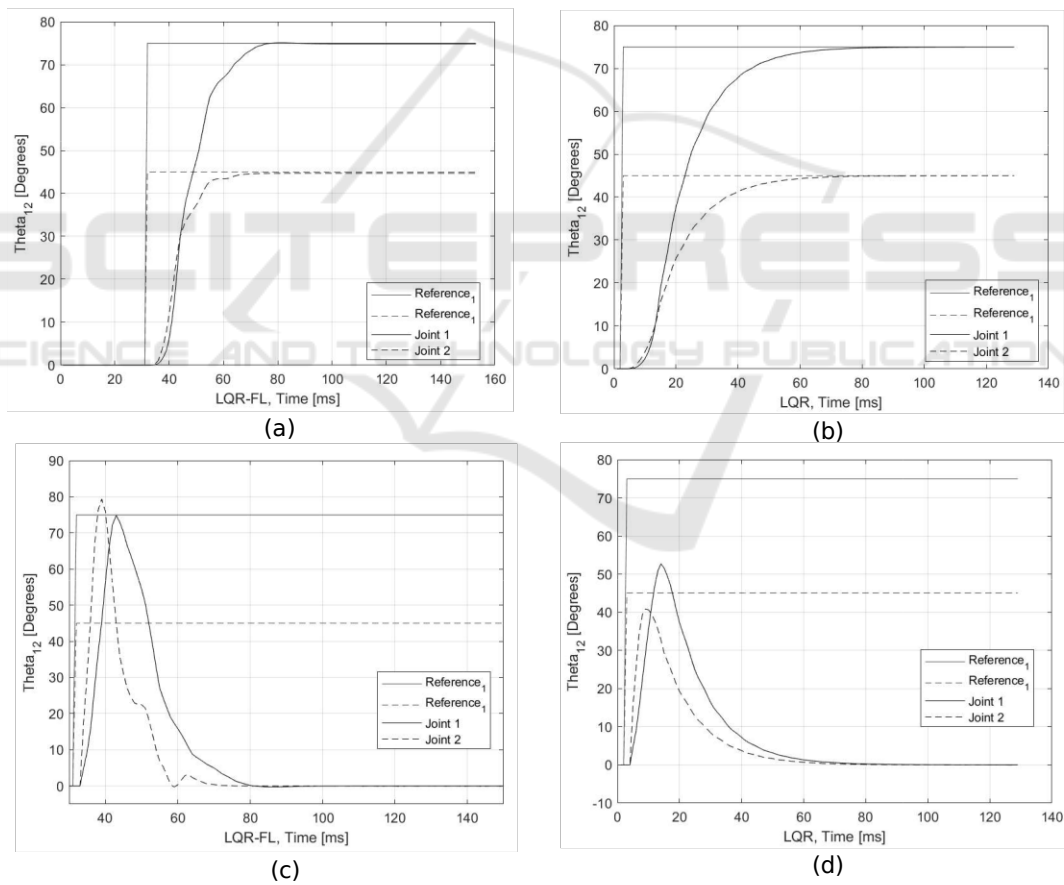


Figure 7: LQR position control.

5 CONCLUSIONS

This study presents a methodology to enhance the precision performance and steady-state behavior of a robotic arm using LQR controller with computational tuning. The LQR-FL hybrid control demonstrated to operate with a smaller trajectory tracking error than the one presented in the traditional LQR controller. Therefore, the computational adjustment of the LQR controller weighting matrices improved the simulation performance in trajectory control.

5.1 Future Research

The performance of the controllers could be compared in consideration of tolerances to disturbances and noise and some comparative stability. An evaluation of the controllers with respect to trajectories of greater complexity is as follows level that is being worked to carry out this investigation.

REFERENCES

- An, T., Zhu, X., Zhu, M., Ma, B., and Dong, B. (2023). Fuzzy logic nonzero-sum game-based distributed approximated optimal control of modular robot manipulators with human-robot collaboration. *Neurocomputing*, 543:126276.
- Bekkar, B. and Ferkous, K. (2023). Design of online fuzzy tuning lqr controller applied to rotary single inverted pendulum: Experimental validation. *Arabian Journal for Science and Engineering*, 48(5):6957–6972.
- Bojan-Dragos, C.-A., Precup, R.-E., Preitl, S., Roman, R.-C., Hedrea, E.-L., and Szedlak-Stinean, A.-I. (2021). Gwo-based optimal tuning of type-1 and type-2 fuzzy controllers for electromagnetic actuated clutch systems. *IFAC-PapersOnLine*, 54(4):189–194.
- García, J. J. A., Castellanos, E. I., and Santana, L. H. (2018). Control por modelo dinámico inverso de simulador de conducción de 2 grados de libertad. *ITEGAM-JETIA*, 4(13):59–65.
- Ho, H., Wong, Y.-K., and Rad, A. B. (2007). Robust fuzzy tracking control for robotic manipulators. *Simulation Modelling Practice and Theory*, 15(7):801–816.
- Kardoš, J. (2019). Robust computed torque method of robot tracking control. In *2019 22nd International Conference on Process Control (PC19)*, pages 102–107. IEEE.
- Kelly, R., Davila, V. S., and Perez, J. A. L. (2005). *Control of robot manipulators in joint space*. Springer Science & Business Media.
- Kudinov, Y., Duvanov, E., Kudinov, I., Pashchenko, A., Pashchenko, F., Pikina, G., Andryushin, A., Arakelyan, E., and Mezin, S. (2020). Construction and analysis of adaptive fuzzy linear quadratic regulator. In *Journal of Physics: Conference Series*, volume 1683, page 042065. IOP Publishing.
- Kumar, A., Raj, R., Kumar, A., and Verma, B. (2023). Design of a novel mixed interval type-2 fuzzy logic controller for 2-dof robot manipulator with payload. *Engineering Applications of Artificial Intelligence*, 123:106329.
- Lee, T. S., Alandoli, E. A., and Vijayakumar, V. (2021). 2-dof robot modelling by simmechanics and pd-fl integrated controller for position control and trajectory tracking. *F1000Research*, 10:1045.
- Li, Y., Liu, G., Hong, T., and Liu, K. (2005). Robust control of a two-link flexible manipulator with quasi-static deflection compensation using neural networks. *Journal of Intelligent and Robotic Systems*, 44:263–276.
- Mahil, S. M. and Al-Durra, A. (2016). Modeling analysis and simulation of 2-dof robotic manipulator. In *2016 IEEE 59th International Midwest Symposium on Circuits and Systems (MWSCAS)*, pages 1–4. IEEE.
- Nguyen, T.-T. (2019). Sliding mode control-based system for the two-link robot arm. *International Journal of Electrical and Computer Engineering (IJECE)*, 9(4):2771–2778.
- Ogata, K. (2010). *Modern control engineering fifth edition*. Prentice Hall.
- Pizarro-Lerma, A., García-Hernández, R., and Santibáñez, V. (2018). Fine-tuning of a fuzzy computed-torque control for a 2-dof robot via genetic algorithms. *IFAC-papersonline*, 51(13):326–331.
- Shah, J., Rattan, S., and Nakra, B. (2011). Kinematic analysis of 2-dof planer robot using artificial neural network. *International Journal of Mechanical and Mechatronics Engineering*, 5(9):1720–1723.
- Song, Z., Yi, J., Zhao, D., and Li, X. (2005). A computed torque controller for uncertain robotic manipulator systems: Fuzzy approach. *Fuzzy sets and systems*, 154(2):208–226.
- Sun, Y., Liang, X., and Wan, Y. (2023). Tracking control of robot manipulator with friction compensation using time-delay control and an adaptive fuzzy logic system. In *Actuators*, volume 12, page 184. MDPI.
- Teng Fong, T., Jamaludin, Z., Bani Hashim, A. Y., and Rahman, M. A. A. (2015). Design and analysis of linear quadratic regulator for a non-linear positioning system. *Applied Mechanics and Materials*, 761:227–232.
- Wahrburg, A. and Listmann, K. (2016). Mpc-based admittance control for robotic manipulators. In *2016 IEEE 55th Conference on Decision and Control (CDC)*, pages 7548–7554. IEEE.